



A LETTERS JOURNAL EXPLORING  
THE FRONTIERS OF PHYSICS

OFFPRINT

**Stick-slip vs. smooth sliding in the  
multicontact interface**

O. M. BRAUN

EPL, 109 (2015) 48004

Please visit the website  
[www.epljournal.org](http://www.epljournal.org)

**Note** that the author(s) has the following rights:

- immediately after publication, to use all or part of the article without revision or modification, **including the EPLA-formatted version**, for personal compilations and use only;
- no sooner than 12 months from the date of first publication, to include the accepted manuscript (all or part), **but not the EPLA-formatted version**, on institute repositories or third-party websites provided a link to the online EPL abstract or EPL homepage is included.

For complete copyright details see: <https://authors.eplletters.net/documents/copyright.pdf>.



A LETTERS JOURNAL EXPLORING  
THE FRONTIERS OF PHYSICS

## AN INVITATION TO SUBMIT YOUR WORK

[www.epljournal.org](http://www.epljournal.org)

### The Editorial Board invites you to submit your letters to EPL

EPL is a leading international journal publishing original, innovative Letters in all areas of physics, ranging from condensed matter topics and interdisciplinary research to astrophysics, geophysics, plasma and fusion sciences, including those with application potential.

The high profile of the journal combined with the excellent scientific quality of the articles ensures that EPL is an essential resource for its worldwide audience. EPL offers authors global visibility and a great opportunity to share their work with others across the whole of the physics community.

### Run by active scientists, for scientists

EPL is reviewed by scientists for scientists, to serve and support the international scientific community. The Editorial Board is a team of active research scientists with an expert understanding of the needs of both authors and researchers.



OVER  
**560,000**  
full text downloads in 2013

**24 DAYS**  
average accept to online  
publication in 2013

**10,755**  
citations in 2013

*"We greatly appreciate  
the efficient, professional  
and rapid processing of  
our paper by your team."*

Cong Lin  
Shanghai University

## Six good reasons to publish with EPL

We want to work with you to gain recognition for your research through worldwide visibility and high citations. As an EPL author, you will benefit from:

- 1 Quality** – The 50+ Co-editors, who are experts in their field, oversee the entire peer-review process, from selection of the referees to making all final acceptance decisions.
- 2 Convenience** – Easy to access compilations of recent articles in specific narrow fields available on the website.
- 3 Speed of processing** – We aim to provide you with a quick and efficient service; the median time from submission to online publication is under 100 days.
- 4 High visibility** – Strong promotion and visibility through material available at over 300 events annually, distributed via e-mail, and targeted mailshot newsletters.
- 5 International reach** – Over 2600 institutions have access to EPL, enabling your work to be read by your peers in 90 countries.
- 6 Open access** – Articles are offered open access for a one-off author payment; green open access on all others with a 12-month embargo.

Details on preparing, submitting and tracking the progress of your manuscript from submission to acceptance are available on the EPL submission website [www.epletters.net](http://www.epletters.net).

If you would like further information about our author service or EPL in general, please visit [www.epjjournal.org](http://www.epjjournal.org) or e-mail us at [info@epjjournal.org](mailto:info@epjjournal.org).

EPL is published in partnership with:



European Physical Society



Società Italiana  
di Fisica

edp sciences IOP Publishing

EDP Sciences

IOP Publishing

# Stick-slip vs. smooth sliding in the multicontact interface

O. M. BRAUN

*Institute of Physics, National Academy of Sciences of Ukraine - 46 Science Avenue, 03028 Kiev, Ukraine*

received 22 October 2014; accepted in final form 11 February 2015  
published online 3 March 2015

PACS 81.40.Pq – Friction, lubrication, and wear  
PACS 46.55.+d – Tribology and mechanical contacts

**Abstract** – The stick-slip and smooth sliding regimes of motion for the multicontact frictional interface are studied within the earthquake-like model. It is shown that the stick-slip appears when two necessary conditions are fulfilled: first, the system must be soft enough for the elastic instability to emerge, and second, it must be ageing of the interface. The stick-slip exists only for an interval of sliding velocities  $v_1 < v_d < v_2$ , where both boundary velocities  $v_{1,2}$  are determined by the ageing rate.

Copyright © EPLA, 2015

**Introduction.** – The regime of motion of the frictional interface —stick-slip or smooth sliding— is a rather old but very important problem in tribology [1,2]. In some situations (for example, for violin playing) stick-slip is a desirable regime, but in the majority of cases (*e.g.*, for windshield wiper, car engine operation, earthquakes, etc.) the stick-slip has to be avoided or suppressed at least. These two regimes, the stick-slip and smooth sliding, and the transitions between them are traditionally described by a phenomenological theory based on the “velocity weakening” assumption [1,2]: if the friction force decreases when the sliding velocity grows, the motion may become unstable and could switch to stick-slip, either periodic or irregular (intermittent) motion. The theory predicts that generally stick-slip emerges for a soft system and low driving velocities. However, a general physical theory of this problem is still lacking.

In the present work we consider a multicontact interface (MCI), when the contact between two surfaces is due to many “frictional” contacts (asperities, bridges, etc.) —a rather general situation in tribology. The MCI may be described by an earthquake-like (EQ) model (based on the famous spring-and-block Burridge and Knopoff model [3] and adapted to the frictional interface, *e.g.*, in refs. [4–6]), which allows an analytical description using the master equation (ME) approach [7,8]. The stick-slip motion in the MCI may appear, *if and only if* two ingredients are incorporated into the model: the elastic instability of the system and ageing of the contacts [9,10]. The aim of the present work is to find the conditions when the stick-slip regime emerges in the multicontact interface.

**EQ model and ME approach.** – The EQ model is shown schematically in fig. 1 (inset). The top block (the slider) is coupled with the bottom block (the base; we assume it to be rigid and fixed) by  $N$  frictional contacts. Each contact is characterized by a shear force  $f_i = kx_i$ , where  $k$  is the contact stiffness<sup>1</sup> and  $x_i$  is its strain, and by a stretching threshold  $x_{si} = f_{si}/k$  at which the contact breaks. The contact thresholds are characterized by some distribution  $P_c(x)$  which is determined by interface structure, *e.g.*, by surface roughness (in simulation we assume that  $P_c(x)$  has the Gaussian shape centered at  $x = x_s = f_s/k$  with a dispersion  $\Delta x_s = \Delta f_s/k$ ). The contact stretches elastically so long as  $|f_i| < f_{si}$ , but breaks when the threshold is exceeded. When a contact breaks, its stretching drops to  $x_i \sim 0$ , and evolution continues from there, with a new value (taken randomly from the distribution  $P_c(x)$ ) for its successive breaking threshold assigned.

The EQ model, being a cellular automaton model, allows a numerical study only. However, it is possible to describe it analytically with the ME approach [7,8]. Introducing the distribution  $Q(x; X)$  of the contact stretchings  $x_i$  when the sliding block is at position  $X$ , evolution of the system can be described by the integro-differential equation (the master equation)

$$\left[ \frac{\partial}{\partial X} + \frac{\partial}{\partial x} + P(x) \right] Q(x; X) = \delta(x) \Gamma(X), \quad (1)$$

<sup>1</sup>We assume that all contacts have the same (average) stiffness  $k$ , although in a more rigorous model their values have to be coupled with the corresponding thresholds,  $k_i \propto f_{si}^{1/2}$  [8–10]; this assumption does not modify our results.

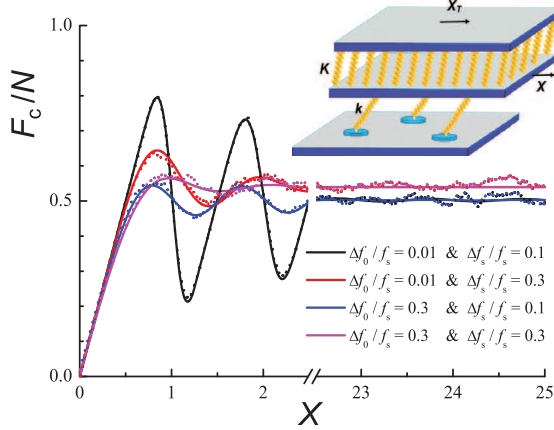


Fig. 1: (Color online) Rigid motion of the slider: the total force from contacts  $F_c$  as a function of the slider displacement  $X$  for two initial distributions  $\Delta f_0/f_s = 0.01$  and  $0.3$  and two values of the threshold distribution  $\Delta f_s/f_s = 0.1$  and  $0.3$  (see legend). Solid curves describe solutions of the master equation, dotted curves show results of simulation of the earthquake-like model with  $N = 10^3$  contacts; the latter fluctuate with the amplitude  $\propto N^{-1/2}$ . Inset: the earthquake-like model.

where we assumed that broken contacts reappear with zero stretching [8],

$$\Gamma(X) = \int_{-\infty}^{\infty} d\xi P(\xi) Q(\xi; X) \quad (2)$$

and

$$P(x) = P_c(x)/J_c(x), \quad J_c(x) = \int_x^{\infty} d\xi P_c(\xi). \quad (3)$$

The master equation should be solved starting from some initial distribution  $Q(x; X=0) = Q_i(x)$ ; in what follows we assume that  $Q_i(x)$  has a Gaussian shape centered at zero with a dispersion  $\Delta x_0 = \Delta f_0/k$ . The total force experienced by the slider from the interface is then given by

$$F_c(X) = Nk \int_{-\infty}^{\infty} dx x Q(x; X). \quad (4)$$

A typical dependence of the force  $F_c$  on the slider displacement  $X$  is shown in fig. 1. Except for the exotic case of the delta-function distribution of thresholds, the system always approaches the steady state with the distribution  $Q_s(x)$  in the limit  $X \rightarrow \infty$ , where the function  $F_c(X)$  takes the constant value  $F_k \approx \frac{1}{2}Nf_s$ . The value  $F_k$  corresponds to the kinetic friction force, while the maximum of the  $F_c(X)$  dependence is associated with the static friction force. We emphasize that the shape of the function  $F_c(X)$  depends on the initial distribution  $Q_i(x)$  of the system: the strongest initial oscillations of  $F_c(X)$  are achieved for the delta-function initial distribution  $Q_i(x) = \delta(x)$ , while in the case of  $Q_i(x) = Q_s(x)$  the force is independent of  $X$ ,  $F_c(X) = F_k$ .

**Elastic instability.** – Now let us consider a system where the top block is driven with a velocity  $v_d$  through

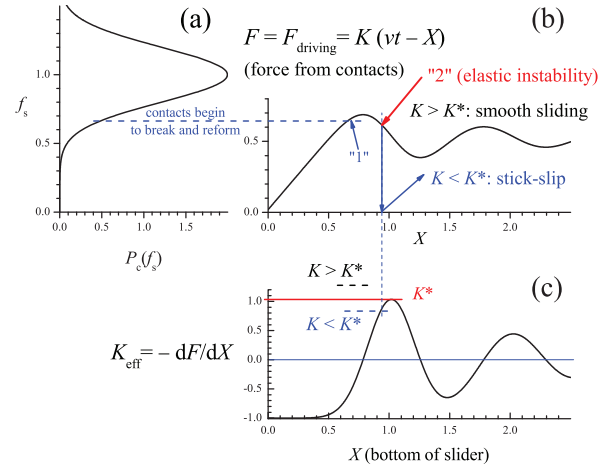


Fig. 2: (Color online) (a) Distribution of thresholds  $P_c(f_s)$ ; (b) the friction force  $F_c$  and (c) the effective stiffness  $K_{\text{eff}}$ , eq. (5), as functions of the displacement  $X$ . Elastic instability emerges when  $K_{\text{eff}}(X^*) = K < K^*$ .

a spring of elastic constant  $K$  so that the driving force is  $F_d = K(v_d t - X)$ ; the role of spring may be played by the elasticity of the slider itself, if the driving force is applied to its top surface. For adiabatically slow driving,  $v_d \rightarrow 0$ , if one starts from the relaxed state at  $t = 0$ , the increasing driving force  $F_d$  has to be compensated by the force  $F_c$  from the interface contacts, so that they grow together at the beginning. However, when the slider displacement  $X$  approaches the threshold value  $x_s$ , the contacts start to break (see the point marked by “1” in fig. 2), the growth of  $F_c$  becomes slower and then changes to decreasing as shown in fig. 2. If the driving spring is stiff enough,  $K > K^*$ , the driving force  $F_d$  will adjust itself to the changed value of  $F_c$ . For a soft system, however, at some point  $X^*$  (marked by “2” in fig. 2) the two forces cannot compensate one another, an elastic instability occurs, and the slider will undergo an accelerated motion until the forces will compensate one another again.

An alternative explanation of the elastic instability follows from the consideration of the effective potential energy of the system. The total force applied to the bottom of the sliding block, which determines its displacement  $X$ , is the sum of the applied force and the friction force,  $F_{\text{tot}}(X) = K(v_d t - X) - F_c(X)$ . It can be viewed as derived from the effective potential,  $F_{\text{tot}}(X) = -dV_{\text{eff}}(X)/dX$ , where  $V_{\text{eff}}(X) = \frac{1}{2}K(v_d t - X)^2 + \int_0^X d\xi F_c(\xi)$ . The slider state at the position  $X$  is stable if  $d^2V_{\text{eff}}(X)/dX^2 = K + dF_c(X)/dX > 0$  and unstable otherwise. If we introduce the effective interface stiffness

$$K_{\text{eff}}(X) = -dF_c(X)/dX, \quad (5)$$

then the slider motion becomes unstable for displacements  $X$  where  $K_{\text{eff}}(X) > K$ . Thus, the critical stiffness is defined by  $K^* = \max K_{\text{eff}}(X)$ . If  $K > K^*$ , the system is stiff and does not undergo elastic instability.

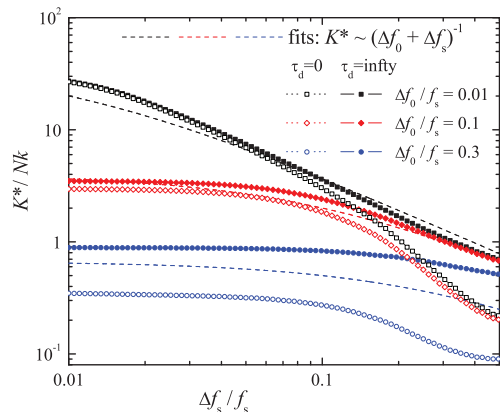


Fig. 3: (Color online) The critical stiffness  $K^*$  as a function of the threshold dispersion  $\Delta f_s$  for different values of the initial state distribution  $\Delta f_0$ .

The critical value  $K^*$  depends on *two factors*: on the threshold distribution  $P_c(x)$  and on the initial distribution  $Q_i(x)$ ; the maximum value of  $K^*$  is achieved for the delta-function initial distribution  $Q_i(x) = \delta(x)$ , while the minimum —equal to zero— for the stationary distribution  $Q_i(x) = Q_s(x)$ . The dependence of  $K^*$  on the model parameters is shown in fig. 3; roughly it is described by

$$K^* \approx Nk f_s / (\Delta f_s + \Delta f_0). \quad (6)$$

**Dynamics.** — The elastic instability is the necessary but not sufficient condition for stick-slip to emerge; the second necessary condition is the ageing of contacts —an increase of contact thresholds with their lifetime. Indeed, if after breaking the newborn contacts obtain thresholds from the same distribution  $P_c(x)$ , then the dependence  $F_c(X)$  will remain approximately unchanged despite the fact that the slider motion is accelerated in the interval where  $K_{\text{eff}}(X) > K^*$  as demonstrated in fig. 4(a).

The simplest way to incorporate contact ageing is to introduce a delay time  $\tau_d$ , *i.e.*, to assume that after breaking the contact reappears after some time  $\tau_d$  (thus, for a lifetime shorter than  $\tau_d$  the threshold is zero). Within the ME approach, the delay effects may be included as follows. Let  $N$  be the total number of contacts,  $N_c$  be the number of attached (pinned) contacts,  $N_f = N - N_c$  be the number of detached (sliding) contacts, and  $v = \dot{X}$  be the sliding velocity. The fraction of contacts that detach per unit displacement of the sliding block is  $\Gamma(X) = \int dx P(x; X) Q(x; X)$ , *i.e.*, when the slider shifts by  $\Delta X$ , the number of detached contacts changes by  $N_c \Gamma \Delta X$ , so that  $N_f = \Gamma v \tau_d N_c$ . Using  $N_c + N_f = N$ , we obtain  $N_c = N / (1 + \Gamma v \tau_d)$  and  $N_f = N \Gamma v \tau_d / (1 + \Gamma v \tau_d)$ . Introducing  $\bar{x} = 1/\Gamma$  and  $\bar{v} = \bar{x}/\tau_d$ , we can write

$$N_c = N / (1 + v/\bar{v}). \quad (7)$$

The pinned contacts produce the force  $F_c(X)$  defined above by eq. (4) (with  $N_c$  instead of  $N$ ) by solution of the master equation.

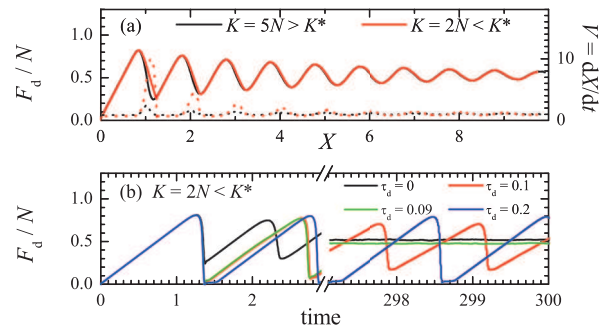


Fig. 4: (Color online) (a) Dependence of the driving force  $F_d$  (solid) and the slider velocity  $\dot{X}$  (dotted curves, right axes) on the slider displacement  $X$  for two values of the spring constant:  $K/N = 5$  (above the critical value  $K^*/N = 3.59$ ) and  $K/N = 2$  (when the elastic instability occurs). (b) Dependence of  $F_d$  on time for different values of the delay time  $\tau_d = 0, 0.09, 0.1$  and  $0.2$  (see legend) for the spring constant  $K/N = 2$ . The parameters are the following:  $f_s = 1$ ,  $\Delta f_s = 0.1$ ,  $\Delta f_0 = 0.01$ ,  $k = 1$ ,  $v_d = 1$ ,  $M/N = 10^{-4}$  (so that  $\Omega = (K/M)^{1/2} = 223.6$  for  $K/N = 5$  and  $\Omega = 141.4$  for  $K/N = 2$ ),  $\eta = 200 \sim \Omega$ , and  $N = 10^4$ .

The slider motion is described by the equation

$$M\ddot{X}(t) + M\eta\dot{X}(t) = K[v_d t - X(t)] - F_c(X(t)), \quad (8)$$

where  $M$  is the slider mass and the coefficient  $\eta$  describes the rate of energy dissipation (*e.g.*, due to phonons emitted inside the slider); the latter is responsible for decaying ringing oscillations at stick-slip and thus can be found experimentally. Figure 4(b) shows that for a large enough delay time  $\tau_d > \tau^*$  the slider motion corresponds to stick-slip provided  $K < K^*$ .

To find the critical delay time  $\tau^*$ , let us consider the slider trajectory just after the critical displacement  $X^*$  (the point “2” in fig. 2), when the elastic instability occurs and the motion becomes unstable. The system dynamics is shown in fig. 5. Before the instability,  $t < t^*$ , the two forces, the driving force  $F_d$  and the force from contacts  $F_c$ , approximately compensate one another, and the slider moves with a constant velocity,  $\dot{X} \approx v_d$ . After  $t^*$ , however, the forces become unbalanced, the difference  $F_{\text{tot}} = F_d - F_c$  grows with  $\Delta t = t - t^*$  (see fig. 5(a)), and the slider undergoes an accelerated motion with increasing velocity (fig. 5(c)). As was found in ref. [10], for  $t > t^*$  the slider position changes as

$$\Delta X(t) \approx v_d \Delta t \left[ 1 + \frac{1}{6} (\Omega \Delta t)^2 \right], \quad (9)$$

where  $\Omega^2 = K/M$ . When the delay time is nonzero, the slider slips a distance  $\Delta X_d = \Delta X(\tau_d)$  during  $\tau_d$ . Therefore, if  $\Delta X_d > \frac{1}{2} \Delta x_s$ , then most of the contacts break and reform with  $f \sim 0$  during the time  $\tau_d$ , and the distribution of stresses shrinks,  $Q(x; t^* + \tau_d) \rightarrow \delta(x)$ . Thus, the next cycle begins with a narrow stress distribution, and the elastic instability will occur again —that is stick-slip.

The critical delay time  $\tau^*$  may be estimated from eq. (9); for  $\Omega \tau^* \ll 1$  this gives  $\tau^* \approx \Delta x_s / v_d$ , while for

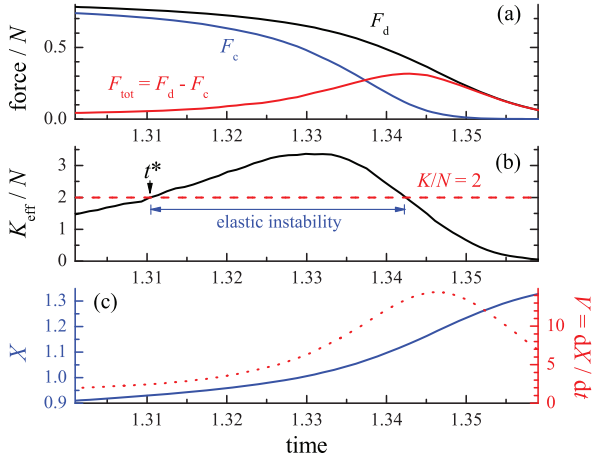


Fig. 5: (Color online) System dynamics at and after the elastic instability for  $K/N = 2$  and  $\tau_d = \infty$  (other parameters as in fig. 4).

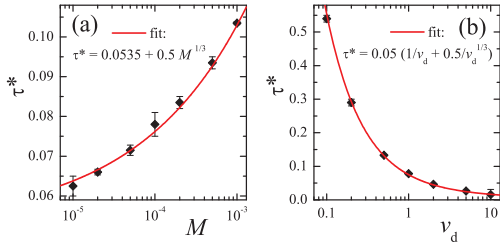


Fig. 6: (Color online) (a) The critical delay time  $\tau^*$  as a function of the slider mass  $M$  at constant  $v_d = 1$ , and (b)  $\tau^*$  as a function of the driving velocity  $v_d$  at fixed  $M = 10^{-4}$ .  $K/N = 2$  and  $\eta = 0.3\Omega$ ; other parameters as in fig. 4.

$\Omega\tau^* \gg 1$  it leads to  $\tau^* \approx (6\Delta x_s M / K v_d)^{1/3}$ . These relations agree well with the numerics (see fig. 6) which suggests the dependences  $\tau^*(M) \approx A_1 + A_2 M^{1/3}$  and  $\tau^*(v_d) \approx A_3 v_d^{-1} + A_4 v_d^{-1/3}$ , where  $A_{1\dots 4}$  are numerical constants. Numerics shows also that  $\tau^*$  increases with the damping coefficient  $\eta$ ;  $\tau^*$  depends also on the parameters  $\Delta f_s$  and  $\Delta f_0$ .

As follows from fig. 6(b), for a fixed nonzero value of the delay time  $\tau_d$  the system should undergo a *transition from smooth sliding to stick-slip when the driving velocity increases*. Such transition is demonstrated in fig. 7(a). The system exhibits hysteresis: when the driving velocity increases, the smooth to stick-slip transition occurs at some velocity  $v_1$ , while when  $v_d$  decreases, the stick-slip to smooth sliding transition occurs at a lower velocity  $v'_1$ . The hysteresis takes place because, as mentioned above, the criterion of the elastic instability to occur, depends on the initial distribution for a given cycle of stick-slip, which depends on the system prehistory. Thus, depending on the system initial state and the model parameters, the motion corresponds to either stick-slip or smooth sliding. These regimes are stable, both correspond to regular motion, in particular, the stick-slip motion is strictly periodic.

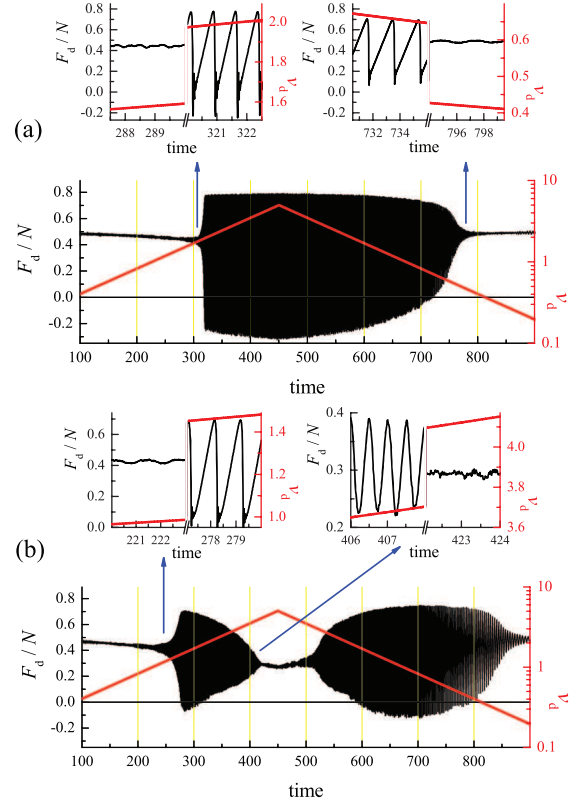


Fig. 7: (Color online) The friction force as a function of time, when the driving velocity  $v_d$  (thick red line, right axes) continuously increases/decreases with time. (a) Fixed value of the delay time  $\tau_d = 0.1$ . (b) Delay time takes random values from Gaussian distribution with  $\langle \tau_d \rangle = 0.2$  and  $\Delta \tau_d = 0.12$ . Insets show the smooth to stick-slip transitions.  $K/N = 2$ ,  $M = 10^{-4}$  and  $\eta = 0.3\Omega$ ; other parameters as in fig. 4.

The simplest “delay time” variant of ageing predicts the transition from smooth sliding to stick-slip with the increase of the driving velocity, as indeed was observed experimentally [11,12]. More traditional, however, is the opposite scenario, when stick-slip is observed at low  $v_d$  and changes to smooth sliding when the driving velocity increases [1,2]. The EQ model does demonstrate such a behavior, if we assume that the parameter  $\tau_d$  takes random values from some distribution  $P_\tau(\tau_d)$  with a dispersion  $\Delta \tau_d$ , as shown in fig. 7(b). Moreover, in this case one may expect an irregular stick-slip as well [13–15]. This second transition occurs because the elastic instability disappears at large velocities —after a slip phase at the stick-slip event, the newborn contacts have the distribution with the dispersion  $\Delta x \propto v_d \Delta \tau_d$  which grows with  $v_d$ .

**Ageing.** – In a more general approach one has to include ageing of the contacts [5]. Indeed, the threshold value of contact after its reattachment should grow with the time of stationary contact, *e.g.*, because of plastic deformations at the level of contacts or a slow formation of chemical bonds.

Although we do not know the actual ageing mechanism, one may assume that the evolution of newborn thresholds

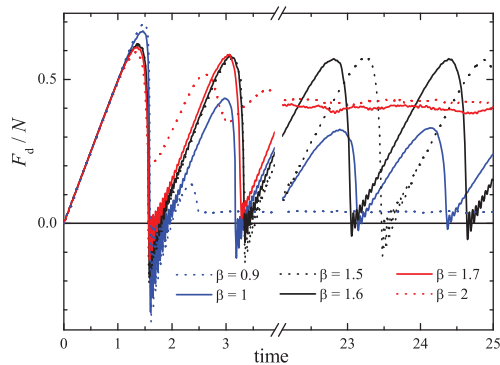


Fig. 8: (Color online) The friction force *vs.* time for different values of the ageing rate  $\beta$  (see legend); stick-slip exists for the rates within the interval  $1 \leq \beta \leq 1.6$ .  $f_s = 1$ ,  $\Delta f_s = 0.1$ ,  $\Delta f_0 = 0.01$ ,  $k = 1$ ,  $N = 2 \times 10^3$ ,  $K/N = 1$ ,  $M = 10^{-4}$ ,  $v_d = 1$  and  $\eta = 0.1\Omega$ .

can be represented as a stochastic process described by the simplest stochastic equation  $df_{si} = H(f_{si}) dt + G dw$  with  $\langle dw \rangle = 0$  and  $\langle dw dw \rangle = dt$ , where  $H(f)$  and  $G$  are the so-called drift and stochastic forces correspondingly [16]. Alternatively, this process is described by the Langevin equation

$$df_{si}(t)/dt = H(f_{si}) + G \xi(t), \quad (10)$$

where  $\xi(t)$  is the Gaussian random force,  $\langle \xi(t) \rangle = 0$  and  $\langle \xi(t) \xi(t') \rangle = \delta(t - t')$ . Equation (10) is equivalent to the Fokker-Planck equation (FPE) for the distribution of thresholds  $P_c(f_{si}; t)$ :

$$\frac{\partial P_c}{\partial t} + \frac{dH}{df_{si}} P_c + H \frac{\partial P_c}{\partial f_{si}} = \frac{1}{2} G^2 \frac{\partial^2 P_c}{\partial f_{si}^2}. \quad (11)$$

Following ref. [17], let us assume that the drift force is given by the expression  $H(f) = \beta^2 (f_s - f)$ , while the amplitude of the stochastic force is equal to  $G = \beta \delta f_s \sqrt{2}$ , where  $\delta \equiv \Delta f_s / f_s$  and  $\beta$  defines the rate of ageing described by the timescale  $\tau_\beta = \beta^{-2}$ . With this choice, the stationary solution  $P_{c0}(f)$  of the FPE corresponds to the Gaussian distribution  $P_{c0}(f) = (2\pi)^{-1/2} (\delta f_s)^{-1} \exp[-\frac{1}{2}(1 - f/f_s)^2 / \delta^2]$ .

The ME approach described above should now be modified, because the distribution  $P_c(x)$  is not fixed but evolve due to ageing of the contacts. Equation (11) describes how the distribution of the thresholds evolves under the effect of ageing alone. This equation may be rewritten as

$$\frac{\partial P_c}{\partial t} = \beta^2 \hat{L} P_c, \quad \hat{L} = \frac{\partial}{\partial \phi} \left( \phi - 1 + \delta^2 \frac{\partial}{\partial \phi} \right), \quad (12)$$

where  $\phi = f/f_s$ . However, because the contacts continuously break and form again when the slider moves, this introduces two extra contributions in the equation determining  $\partial P_c / \partial t$  in addition to the pure aging effect described by eq. (12): a term  $P(x; X) Q(x; X)$  takes into account the contacts that break, while their reappearance with the threshold distribution  $P_{ci}(x)$  (e.g.,  $P_{ci}(x) = \delta(x)$ )

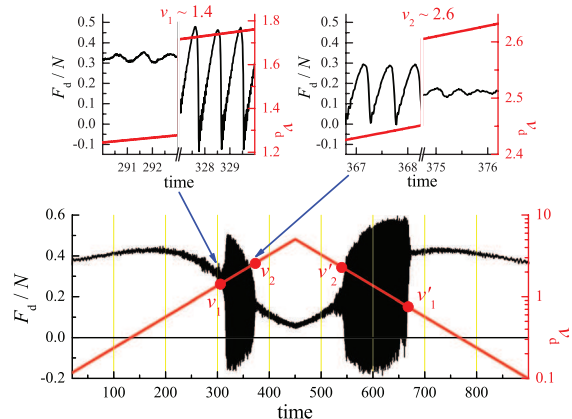


Fig. 9: (Color online) The friction force as a function of time, when the driving velocity  $v_d$  (thick red line, right axes) continuously increases/decreases with time. The insets show the smooth to stick-slip transition at  $v_1$  and the stick-slip to smooth sliding transition at  $v_2$  when  $v_d$  increases.  $\beta = 1.5$ , other parameters as in fig. 8.

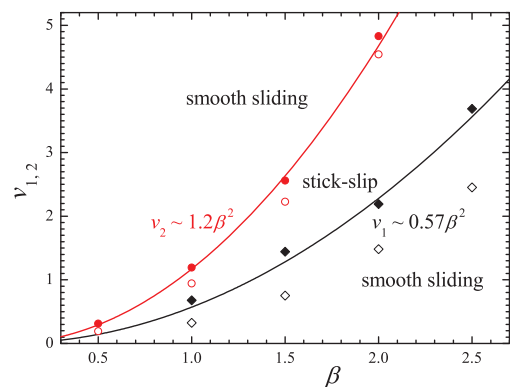


Fig. 10: (Color online) The critical velocities  $v_{1,2}$  (solid symbols) and  $v'_{1,2}$  (open symbols) as functions of the ageing rate  $\beta$ . Solid curves show fits  $v_{1,2} \propto \beta^2$ . The parameters are as in fig. 9.

gives rise to the second extra term in the equation. Therefore, the full evolution of  $P_c(x; X)$  is described by the equation

$$\frac{\partial P_c(x; X)}{\partial X} - \frac{\beta^2}{v} \hat{L} P_c(x; X) + P(x; X) Q(x; X) = P_{ci}(x) \Gamma(X). \quad (13)$$

In the result we come to the set of equations (1)–(3), (13).

If now one drives the slider through an attached spring, then the motion may correspond to either stick-slip or smooth sliding depending on the rate  $\beta$ ; the stick-slip regime appears for the rates within some interval  $\beta_1 \leq \beta \leq \beta_2$ , while for smaller or larger values of  $\beta$  the motion is smooth (see fig. 8).

Thus, when the driving velocity continuously increases, the system should undergo two transitions, the smooth to stick-slip transition at  $v_1$  and the stick-slip to smooth sliding transition at  $v_2$ ; if then  $v_d$  decreases, one again observes two transitions at  $v'_2$  and  $v'_1$  (see fig. 9). The critical velocities  $v_1$  and  $v_2$  depend on the ageing rate  $\beta$  as

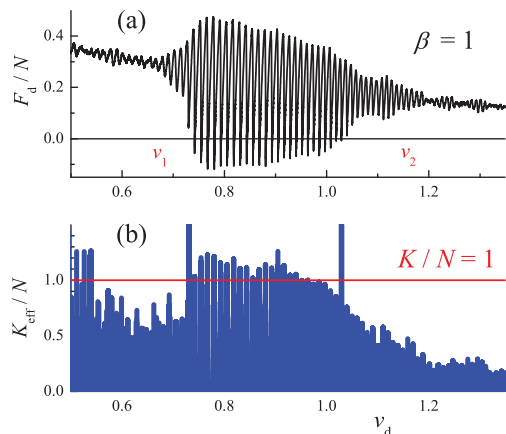


Fig. 11: (Color online) (a) The friction force and (b) the effective stiffness  $K_{\text{eff}}$  as functions of the driving velocity  $v_d$  for the ageing rate  $\beta = 1$ . The parameters are as in fig. 9.

$v_{1,2} \propto \beta^2$  (fig. 10). Both transitions may be explained in the same way as above, if we remind that  $\tau_\beta \sim \tau_d$ : the first transition at  $v_1$  occurs when  $\tau_\beta > \tau^*$  (provided the instability criterion is satisfied), while the second transition at  $v_2$  takes place when the elastic instability disappears (see fig. 11).

**Conclusion.** – We presented the detailed study of the stick-slip behavior of the multicontact interface described by the earthquake-like model. The stick-slip emerges because of two factors, both of which are the necessary conditions. First, the driving spring must be soft enough for the elastic instability to emerge. Second, it must be ageing of the interface—the growth of the static threshold with the lifetime of the stationary contact. The first factor is controlled by the dispersion  $\Delta x_s$  of the distribution  $P_c(x)$  of the static thresholds. Therefore, using the interface with a large value of  $\Delta f_s/f_s$ , one may avoid the elastic instability and thus stick-slip. Besides, the value  $K^*$  also depends on the distribution of stretchings in the initial state—if one starts with the stationary distribution  $Q_s(x)$ , the system will stay in the smooth sliding regime forever. Because of the second factor—the contact ageing—the stick-slip exists only for the interval of sliding velocities  $v_1 < v_d < v_2$ ; both boundary velocities  $v_{1,2}$  depend on the ageing rate  $\beta$  as  $v_{1,2} \propto \beta^2$ . Therefore, the stick-slip may also be avoided by an appropriate choice of the operating velocities.

Contrary to the phenomenological approach widely used in the description of the stick-slip behavior, our approach

is based on the model with well-defined parameters which may be measured experimentally and even calculated from first principles. However, a weak point of our approach is that we do not know the actual ageing mechanism. Although it is quite hard to study this slow dynamics experimentally as well as with simulation, the problem of interface ageing is very important not only for tribology, but for other topics such as, *e.g.*, seismology [17].

\*\*\*

We thank M. PEYRARD for helpful discussion. This work was supported by the EGIDE/Dnipro grant No. 28225UH and the NASU “RESURS” program.

## REFERENCES

- [1] PERSSON B. N. J., *Sliding Friction: Physical Principles and Applications* (Springer-Verlag, Berlin) 1998.
- [2] BRAUN O. M. and NAUMOVETS A. G., *Surf. Sci. Rep.*, **60** (2006) 79.
- [3] BURRIDGE R. and KNOPOFF L., *Bull. Seismol. Soc. Am.*, **57** (1967) 341.
- [4] PERSSON B. N. J., *Phys. Rev. B*, **51** (1995) 13568.
- [5] BRAUN O. M. and RÖDER J., *Phys. Rev. Lett.*, **88** (2002) 096102.
- [6] FILIPPOV A. E., KLAFTER J. and URBACH M., *Phys. Rev. Lett.*, **92** (2004) 135503.
- [7] BRAUN O. M. and PEYRARD M., *Phys. Rev. Lett.*, **100** (2008) 125501.
- [8] BRAUN O. M. and PEYRARD M., *Phys. Rev. E*, **82** (2010) 036117.
- [9] BRAUN O. M. and TOSATTI E., *EPL*, **88** (2009) 48003.
- [10] BRAUN O. M. and TOSATTI E., *Philos. Mag.*, **91** (2011) 3253.
- [11] YOSHIZAWA H., MCGUIGGAN P. and ISRAELACHVILI J., *Science*, **259** (1993) 1305.
- [12] RICHETTI P., DRUMMOND C., ISRAELACHVILI J., IN M. and ZANA R., *Europhys. Lett.*, **55** (2001) 653.
- [13] BAREL I., URBACH M., JANSEN L. and SCHIRMEISEN A., *Phys. Rev. Lett.*, **104** (2010) 066104.
- [14] CAPOZZA R. and URBACH M., *Phys. Rev. B*, **86** (2012) 085430.
- [15] BRÖRMANN K., BAREL I., URBACH M. and BENNEWITZ R., *Tribol. Lett.*, **50** (2013) 3.
- [16] GARDINER C. W., *Handbook of Stochastic Methods for Physics, Chemistry and the Natural Sciences* (Springer-Verlag, Berlin) 2004.
- [17] BRAUN O. M. and PEYRARD M., *Phys. Rev. E*, **87** (2013) 032808.